Supporting Information

Microporous Titania Crystals with Penta-oxygen Coordination

Sicong Ma, Si-Da Huang, Ya-Hui Fang and Zhi-Pan Liu*

Email: zpliu@fudan.edu.cn

Collaborative Innovation Center of Chemistry for Energy Material, Shanghai Key Laboratory of Molecular Catalysis and Innovative Materials, Key Laboratory of Computational Physical Science, Department of Chemistry, Fudan University, Shanghai 200433, China

Calculation details

1. TiO_2 global potential energy surface

To map out the TiO_2 global potential energy surface (PES), more than 10^4 TiO_2 structures (10^3 minima) are first visited based on the Stochastic Surface Walking (SSW) global optimization method (see our previous work for detailed methodology of SSW[1-3]) as integrated with first principles DFT calculations. The SSW method is able to explore complex PES to identify unexpected new structures, which has been successfully applied in solid, molecules, clusters.[4-6] Based on the big data of these TiO_2 structures (including the structure coordinates (***q***), DFT energy (***E***), DFT force (***F***)), we utilize the Neural Network (NN) to fit the relationship between the ***q*** and ***E***.[7,8] While the NN PES can achieve comparable accurarcy with DFT PES, the NN calculations in large systems (e.g. > 48 atom) is generally more than 1000 times faster than that using DFT. We utilize the NN potential to explore the PES of TiO_2, more than 10^6 minima can be collected. The minima on the PES can be distinguished by using a distance-weighted Steinhardt-type order parameter (OP).[9,10] The PES of TiO_2 phases is finally obtained, as shown in the E–OP contour plot in Figure S1. More details on the global PES of TiO_2 can be found in Ref. 7.

2. DFT calculation details

All energetic reported in this work were calculated using the plane wave DFT program, Vienna ab initio simulation package VASP,[11] where electron−ion interaction was represented by the projector augmented wave (PAW) [12,13] pesudopotential and the exchange-correlation functional utilized was GGA-PBE.[14] The valence electrons considered are 3p, 3d, 4s for Ti and 2s, 2p for O. The plane wave cutoff energy utilized was 500 eV and a Monkhorst-Pack-scheme k-point meshes of (4 × 4 × 4) was used for First Brillouin-Zone sampling. For all the crystal structures, both lattice and atomic coordinates were fully optimized until the maximal force component below 0.01 eV/Å and the stress below 0.01 GPa. The hybrid HSE06 functional[15] was also utilized to check the relative energy of all the crystal phases (see Figure S3). The first principles molecular dynamics simulation with isothermal-isobaric (NPT) ensembles is performed by using the SIESTA packages, respectively. For the SIESTA, the numerical atomic orbital basis sets and Troullier Martins norm-conserving pseudopotentials are used.[16-18] The semi-core 3s and 3p states of Ti were included. The cutoff for the real space grid was set as 150 Ry.

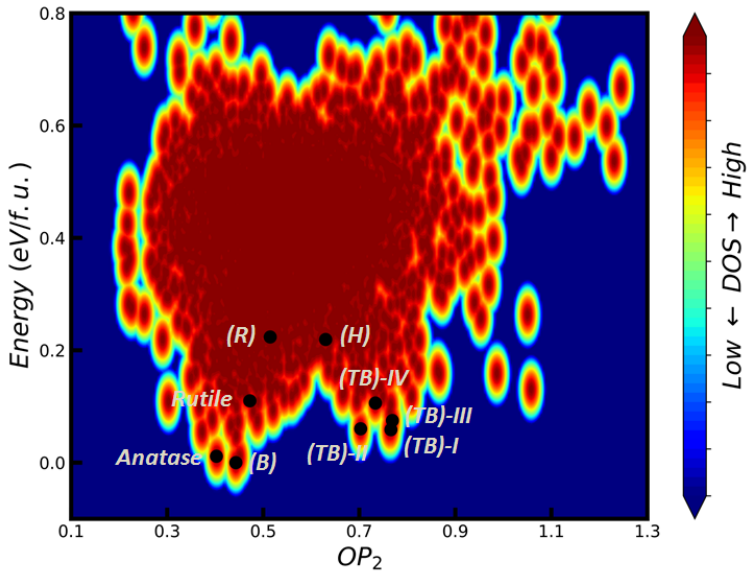

Figure S1. Global PES contour plot for TiO_2 distinct minima sampled from 48-atom ($16TiO_2$) SSW-NN global search (also see Ref. 7 for details). The X-axis is the distance-weighted Steinhardt-type order parameter with the angular moment *l*=2 and the Y-axis is the relative energy of TiO_2 structures with respect to the most stable TiO_2(B) phase. The density of state (DOS) is Boltzmann-weighted density of state as obtained from SSW trajectory.

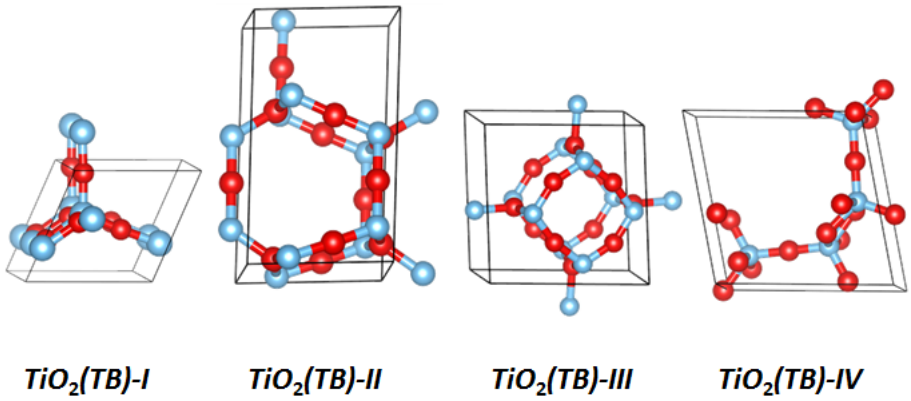

Figure S2. The crystal structures for four different microporous TiO_2(TB) phases. The light blue and red atoms are Ti and O, respectively.

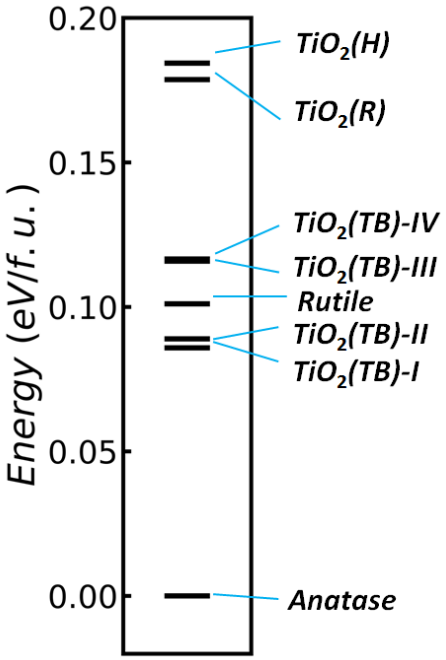

Figure S3. Energy spectrum for TiO_2 crystals from HSE06 functional (anatase is set as the energy reference).

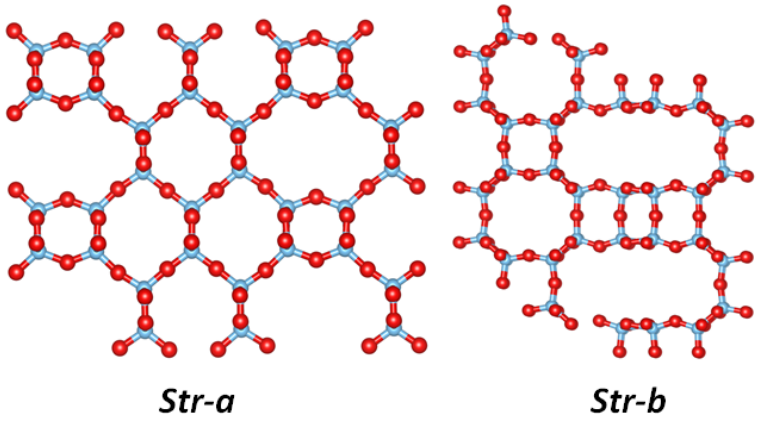

Figure S4. Other possible TiO_2(TB) crystal structures as found from the global PES data. The energies of Str-a and Str-b are 0.05 and 0.16 eV/f.u. relative to anatase calculated with PBE functional, respectively.

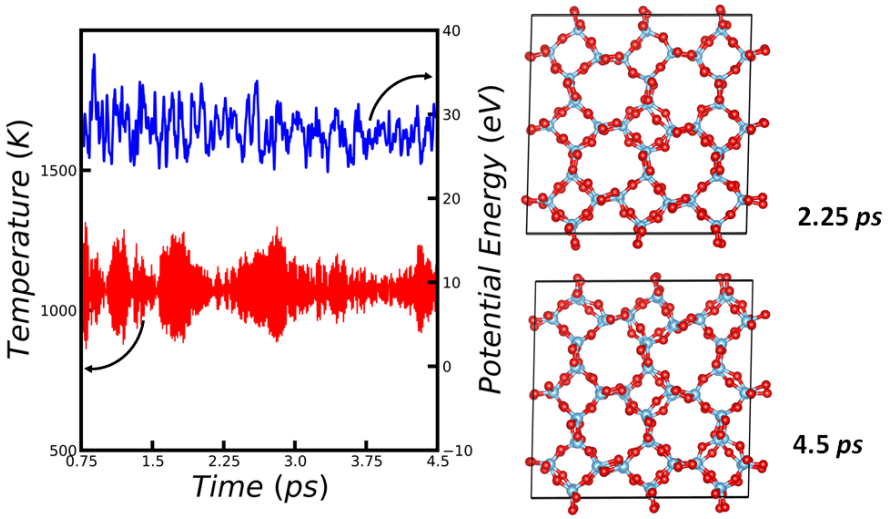

Figure S5. First principles MD simulation with NVT ensemble of TiO_2(TB)-III crystal at 1073 K together with the snapshots at 2.25 and 4.5 ps.

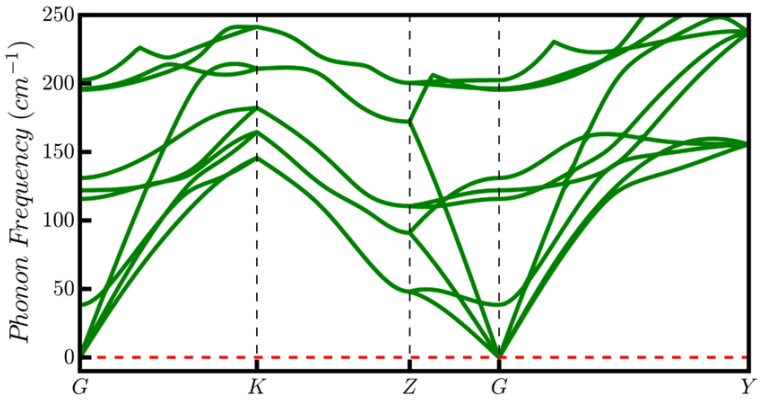

Figure S6. The phonon band structures of TiO_2(TB)-I. High-symmetric k-point paths: G(0,0,0) → K(0.306, -0.306,0.5) → Z(0, 0, 0.5) → G(0, 0, 0) → Y(0.5, 0.5, 0)

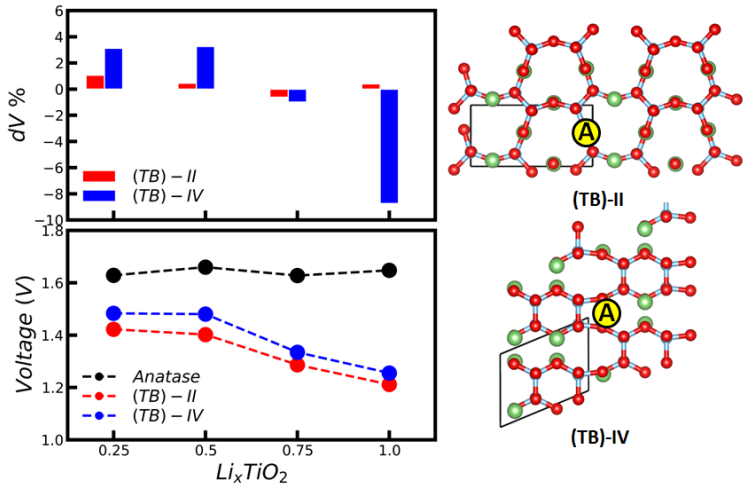

Figure S7. Performance of TiO_2(TB)-II and -IV as Li-ion battery anode at different Li fraction. (Left-top): Plot for volume change *dV* % against Li fraction; (Left-bottom): Plot for the average voltage V_0 against Li fraction; (Right):The structures of Li_xTiO_2(TB)-II and –IV at x = 1. Li atom: Green ball.

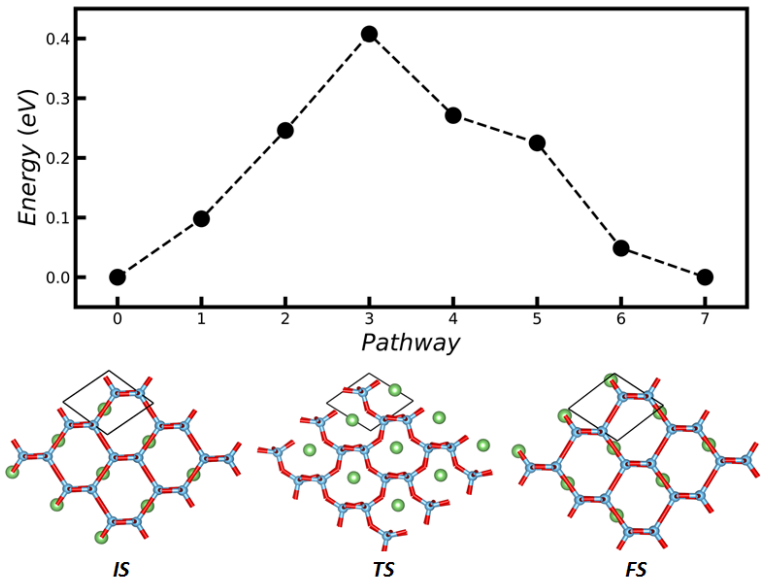

Figure S8. Li ion diffusion energetics in the lowest energy pathway for $Li_{0.25}TiO_2$(TB)-I system.

Table S1. Geometry, Electronic structure and Relative Energies for the Selected TiO_2 Crystalline Phases.

Structure	Anatase	Rutile	TiO_2(R)	TiO_2(H)	TiO_2(TB-I)	TiO_2(TB-II)	TiO_2(TB-III)	TiO_2(TB-IV)
Space group	$I4_1/amd$	$P4_2/mnm$	Pbnm	I4/m	Imma	Cmcm	I4/mmm	Imma
Group #	141	136	62	87	74	63	139	74
Density (g/cm^3)	3.75	4.11	3.46	3.35	2.63	2.54	2.44	2.27
a (Å)	3.82	4.66	9.60	10.31	6.07	3.82	10.69	11.93
b (Å)	3.82	4.66	3.16	10.31	3.82	10.91	10.69	3.81
c (Å)	9.7	5.94	5.06	2.98	9.02	10.03	3.81	10.21
α =β = γ (°)	90	90	90	90	90	90	90	90
CN(Ti)[a]	6	6	6	6	5	5	5	5
CN(O)	3	3	3	3	2	2	2	2
Pore size (Å)	—	—	3.64	5.37	5.77	5.65	6.16	6.71
ΔE[b] (eV/f.u.)	0	0.09	0.16	0.16	0.02	0.02	0.03	0.07
Bulk modulus[c] (GPa)	182.8	219.6	124.5	99.2	120.3	127.3	111.5	83
Band type	Indirect	Direct	Indirect	Indirect	Direct	Indirect	Indirect	Indirect
E_g (eV)[d]	3.33	3.02	3.74	3.80	3.88	3.91	3.86	4.06

[a] coordinate number; [b] relative to the energy of anatase; [c] exp. results: 178 GPa (anatase), 212 GPa (rutile);[19,20] [d] exp. results: 3.2 eV (anatase), 3.0 eV (rutile)

Table S2 The Hirshfeld net atomic populations of different TiO_2 crystals.

	Anatase	Rutile	(R)	(H)	(TB)-I	(TB)-II	(TB)-III	(TB)-IV
Ti	0.688	0.684	0.677	0.677	0.703	0.704	0.706	0.704
O	-0.344	-0.342	-0.338	-0.338	-0.351	-0.352	-0.353	-0.352

TiO_2(TB-I)

system

1.00000000

6.017900000	0.000000000	0.000000000
0.000000000	3.802000000	0.000000000
0.000000000	0.000000000	9.023800000

O Ti

8 4

Direct

0.499997747	0.250001634	0.415804581
0.499997747	0.750004901	0.584195408
-0.000000000	0.750004901	0.915804575
-0.000000000	0.250001634	0.084195413
0.749996620	0.250001634	0.749999991
0.249998874	0.750004901	0.249999997
0.249998874	0.250001634	0.749999991
0.749996620	0.750004901	0.249999997
0.499997747	0.750004901	0.363385758
0.499997747	0.250001634	0.636614230
-0.000000000	0.250001634	0.863385752
-0.000000000	0.750004901	0.136614236

TiO_2(TB-II)

system

1.00000000

3.806800000	0.000000000	0.000000000
0.000000000	10.804500000	0.000000000
0.000000000	0.000000000	10.032400000

O Ti

16 8

Direct

0.499995998	0.499999734	0.000000000
0.499995998	0.499999734	0.500000007
0.000000000	0.000000000	0.000000000
-0.000000000	-0.000000000	0.500000007
0.499995998	0.345163547	0.750000010
0.499995998	0.654835921	0.250000003
-0.000000000	0.845163282	0.750000010
-0.000000000	0.154836187	0.250000003
-0.000000000	0.307747862	0.956773059
-0.000000000	0.692251607	0.043226954
-0.000000000	0.692251607	0.456773053
-0.000000000	0.307747862	0.543226960
0.499995998	0.807747596	0.956773059
0.499995998	0.192251872	0.043226954
0.499995998	0.192251872	0.456773053
0.499995998	0.807747596	0.543226960
0.499995998	0.655828311	0.068623777
0.499995998	0.344171157	0.931376236
0.499995998	0.344171157	0.568623784
0.499995998	0.655828311	0.431376229
-0.000000000	0.155828577	0.068623777
-0.000000000	0.844170891	0.931376236
-0.000000000	0.844170891	0.568623784
-0.000000000	0.155828577	0.431376229

TiO_2(TB-III)

system

1.00000000

10.631800000	0.000000000	0.000000000
0.000000000	10.631800000	0.000000000
0.000000000	0.000000000	3.814800000

O Ti

16 8

Direct

0.301178658	0.499998186	0.500000009
0.698817363	0.499998158	0.500000016
0.499997979	0.301178945	0.499999987
0.499997967	0.698817403	0.500000001
0.801177305	0.000000034	1.000000003
0.198819379	0.000000033	1.000000002
0.999996146	0.801177019	0.000000014
-0.000000013	0.198819375	0.000000000
0.699220370	0.300775613	1.000000003
0.300775413	0.699220388	0.000000003
0.699220400	0.699220439	0.000000004
0.300775749	0.300775832	1.000000001
0.199222234	0.800774163	0.500000007
0.800774230	0.199222526	0.499999999
0.199222305	0.199222346	0.500000002
0.800773865	0.800773861	0.499999999
0.668495225	0.331500888	0.500000004
0.331500779	0.668495392	0.500000005
0.668495138	0.668495280	0.500000007
0.331500908	0.331501010	0.499999997
0.168496999	0.831499209	0.000000005
0.831499251	0.168497197	1.000000003
0.168497208	0.168497146	1.000000005
0.831498998	0.831499166	1.000000004

TiO_2(TB-IV)

1.00000000

8.035300000	0.000000000	0.000000000
-1.596854796	7.875030213	0.000000000
-0.894703447	0.733472661	3.627160796

O Ti

8 4

Direct

0.072007906	0.409412419	0.863687519
0.119972049	0.145023899	0.519803576
0.388964585	0.226354544	0.113963132
0.970283167	0.995390005	0.019901346
0.657954399	0.307718838	0.707996013
0.705921213	0.043331366	0.364010259
0.888986939	0.726374541	0.613968134
0.807643322	0.457358569	0.207899700
0.912886952	0.962018208	0.507969144
0.624586661	0.250301239	0.220032333
0.153343182	0.202438524	0.007766671
0.865045441	0.490731685	0.719831181

References

(1) Shang, C.; Liu, Z.-P. Constrained Broyden minimization combined with the dimer method for locating transition state of complex reactions. *J. Chem. Theory Comp.* **2010**, *6*, 1136-1144.

(2) Shang, C.; Liu, Z.-P. Stochastic surface walking method for structure prediction and pathway searching. *J. Chem. Theory Comp.* **2013**, *9*, 1838-1845.

(3) Zhang, X.-J.; Shang, C.; Liu, Z.-P. From atoms to fullerene: stochastic surface walking solution for automated structure prediction of complex material. *J. Chem. Theory Comp.* **2013**, *9*, 3252-3260.

(4) Guan, S.-H.; Zhang, X.-J.; Liu, Z.-P. Energy landscape of zirconia phase transitions. *J. Am. Chem. Soc.* **2015**, *137*, 8010-8013.

(5) Zhu, S.-C.; Xie, S.-H.; Liu, Z.-P. Nature of rutile nuclei in anatase-to-rutile phase transition. *J. Am. Chem. Soc.* **2015**, *137*, 11532-11539.

(6) Li, Y.-F.; Zhu, S.-C.; Liu, Z.-P. Reaction Network of Layer-to-Tunnel Transition of MnO_2. *J. Am. Chem. Soc.* **2016**, *138*, 5371-5379.

(7) Huang, S.-D.; Shang, C.; Zhang, X.-J.; Liu, Z.-P. Material discovery by combining stochastic surface walking global optimization with a neural network. *Chem. Sci.* **2017**, *8*, 6327-6337.

(8) Behler, J. Atom-centered symmetry functions for constructing high-dimensional neural network potentials. *J. Chem. Phys.* **2011**, *134*, 074106.

(9) Steinhardt, P. J.; Nelson, D. R.; Ronchetti, M. Bond-orientational order in liquids and glasses. *Phys. Rev. B* **1983**, *28*, 784.

(10) Zhang, X.-J.; Shang, C.; Liu, Z.-P. Pressure-induced silica quartz amorphization studied by iterative stochastic surface walking reaction sampling. *Phys. Chem. Chem. Phys.* **2017**, *19*, 4725-4733.

(11) Kresse, G.; Furthmüller, J. Efficient iterative schemes for ab initio total-energy calculations using a plane-wave basis set. *Phys. Rev. B* **1996**, *54*, No. 11169.

(12) Blöchl, P. E. Projector augmented-wave method. *Phys. Rev. B* **1994**, *50*, No. 17953.

(13) Kresse, G.; Joubert, D. From ultrasoft pseudopotentials to the projector augmented-wave method. *Phys. Rev. B* **1999**, *59*, No. 1758.

(14) Perdew, J. P.; Burke, K.; Ernzerhof, M. Generalized gradient approximation made simple. *Phys. Rev. Lett.* **1996**, *77*, No. 3865.

(15) Heyd, J.; Scuseria, G. E.; Ernzerhof, M. Hybrid functionals based on a screened Coulomb potential. *J. Chem. Phys.* **2003**, *118*, 8207-8215.

(16) Sánchez‐Portal, D.; Ordejon, P.; Artacho, E.; Soler, J. M. Density‐functional method for very large systems with LCAO basis sets. *Int. J. Quantum Chem.* **1997**, *65*, 453-461.

(17) Junquera, J.; Paz, Ó.; Sánchez-Portal, D.; Artacho, E. Numerical atomic orbitals for linear-scaling calculations. *Phys. Rev. B* **2001**, *64*, No. 235111.

(18) Soler, J. M.; Artacho, E.; Gale, J. D.; García, A.; Junquera, J.; Ordejón, P.; Sánchez-Portal, D. The SIESTA method for ab initio order-N materials simulation. *J. Phys.: Condens. Matter* **2002**, *14*, No. 2745.

(19) Yao, H.; Ouyang, L.; Ching, W. Y. Ab initio calculation of elastic constants of ceramic crystals. *J. Am. Ceram. Soc.* **2007**, *90*, 3194-3204.

(20) Swamy, V.; Gale, J.; Dubrovinsky, L. Atomistic simulation of the crystal structures and bulk moduli of TiO_2 polymorphs. *J. Phys. Chem. Solids* **2001**, *62*, 887-895.